ASTROBIOLOGY
Volume 2, Number 3, 2002

Application of Hyperspectral Infrared Analysis of Hydrothermal Alteration on Earth and Mars

MATILDA THOMAS* and MALCOLM R. WALTER

ABSTRACT

An integrated analysis of both airborne and field short-wave infrared hyperspectral measurements was used in conjunction with conventional field mapping techniques to map

and supported by thin-section analyses, were used to verify the mineral maps and enhance the level of information obtainable from the airborne data. Hydrothermal alteration zones were identified and mapped separately from the background weathering signals. A main zone of alteration, coinciding with the Paralana Fault zone, was recognized, and found to contain kaolinite, muscovite, biotite, and K-feldspar. A small spectral variation associated with a ring-like feature around Mount Painter was tentatively determined to be halloysite and interpreted to represent a separate hydrothermal fluid and fluid source, and probably a separate system. The older parts of the alteration system are tentatively dated as Permo-Carboniferous. The remote sensing of alteration at Mount Painter confirms that hyperspectral imaging techniques can produce accurate can rl ig22 (s) 42]T1 0 0c1 1672

tulate that a similar exploration strategy would be highly effective on Mars, in that case using satellite and robotic rover-mounted instruments.

Spectroscopy is the measurement and analysis of portions of the electromagnetic spectrum to identify spectrally distinct and physically significant features of a material (Fig. 1). Spectral data are measured using spectral sensors, which record radiation (usually solar) reflected from the surface of materials. Because many materials absorb radiation at specific wavelengths, it is possible to identify them by characteristic absorption features, which appear as troughs in a spectral curve (Kruse, 1994).

Wavelength ranges most suitable for the discrimination of geological materials include the visible and near-infrared (VNIR), SWIR, and the mid- or thermal infrared (TIR) (Fig. 2). Spectral variation is the result of different compositions, the degree of ordering, mixtures, and the grain size of different rocks and minerals (Table 1) (Huntington, 1996). Owing to their multiple valence states, transition elements, such as Fe, Cu, Ni, Cr, Co, Mn, V, Ti, and Sc, display the most prominent spectral features in the VNIR wavelength range (Kruse, 1994).

The SWIR wavelength region between 2,000 and 2,500 nm is particularly suitable for mineral mapping. The 2,000–2,400 nm wavelength region can show many absorption features characteris-the

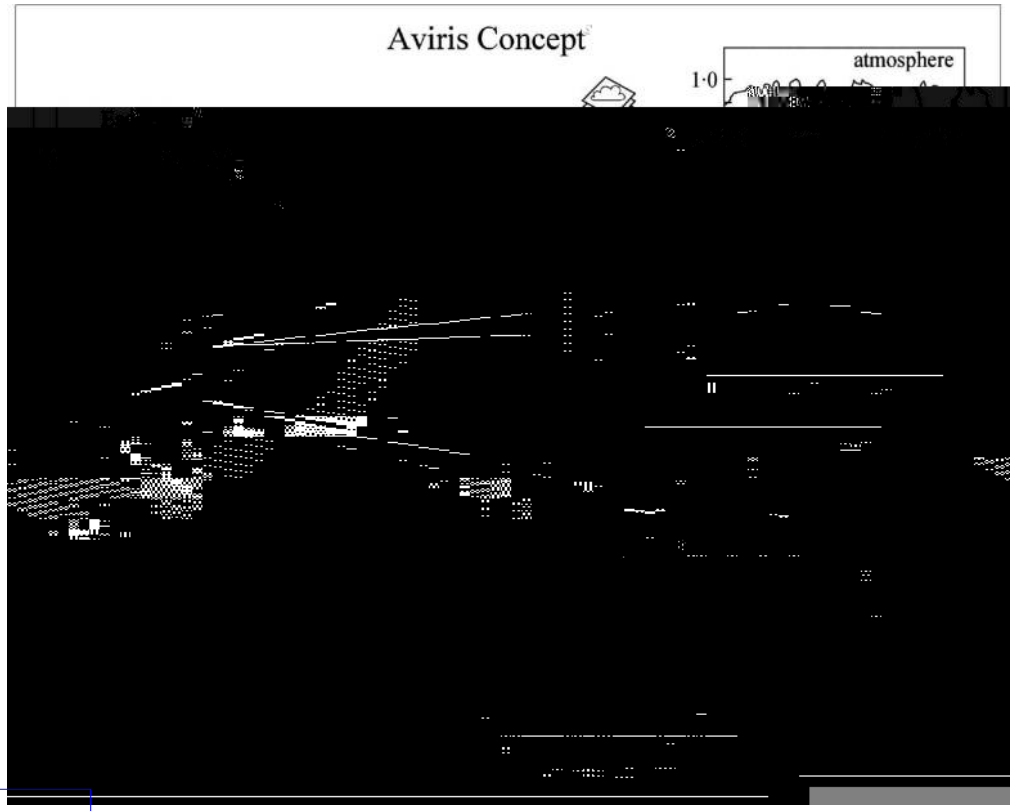

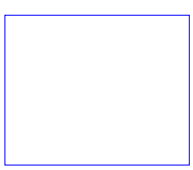

alteration in both ancient and active environments (Yang et al., 2000).

GEOLOGY OF THE MOUNT PAINTER REGION

The Mount Painter Province is located in the northern Flinders Ranges, South Australia, at the northeastern margin of the Neoproterozoic-Cambrian Adelaide Rift Complex (Fig. 3). At present the ranges comprise an elevated, rugged terrain rising from the plains of Lake Frome in the east, eventually merging into the plains of the Great Artesian Basin to the north.

The Mount Babbage and Mount Painter Inliers, together with the Broken Hill and Olary Domains, make up the Curnamona Province. This region is an extensional, probably back arc, continental margin magmatic area of Paleoproterozoic to Mesoproterozoic age. Neoproterozoic-Cambrian clastic sedimentary and carbonate rocks of the Adelaide Rift Complex unconformably overlie the older succession (Foster et al., 1994). The Mount Painter Inlier comprises crystalline basement rocks, the Mount Painter complex, which includes Palaeo- to

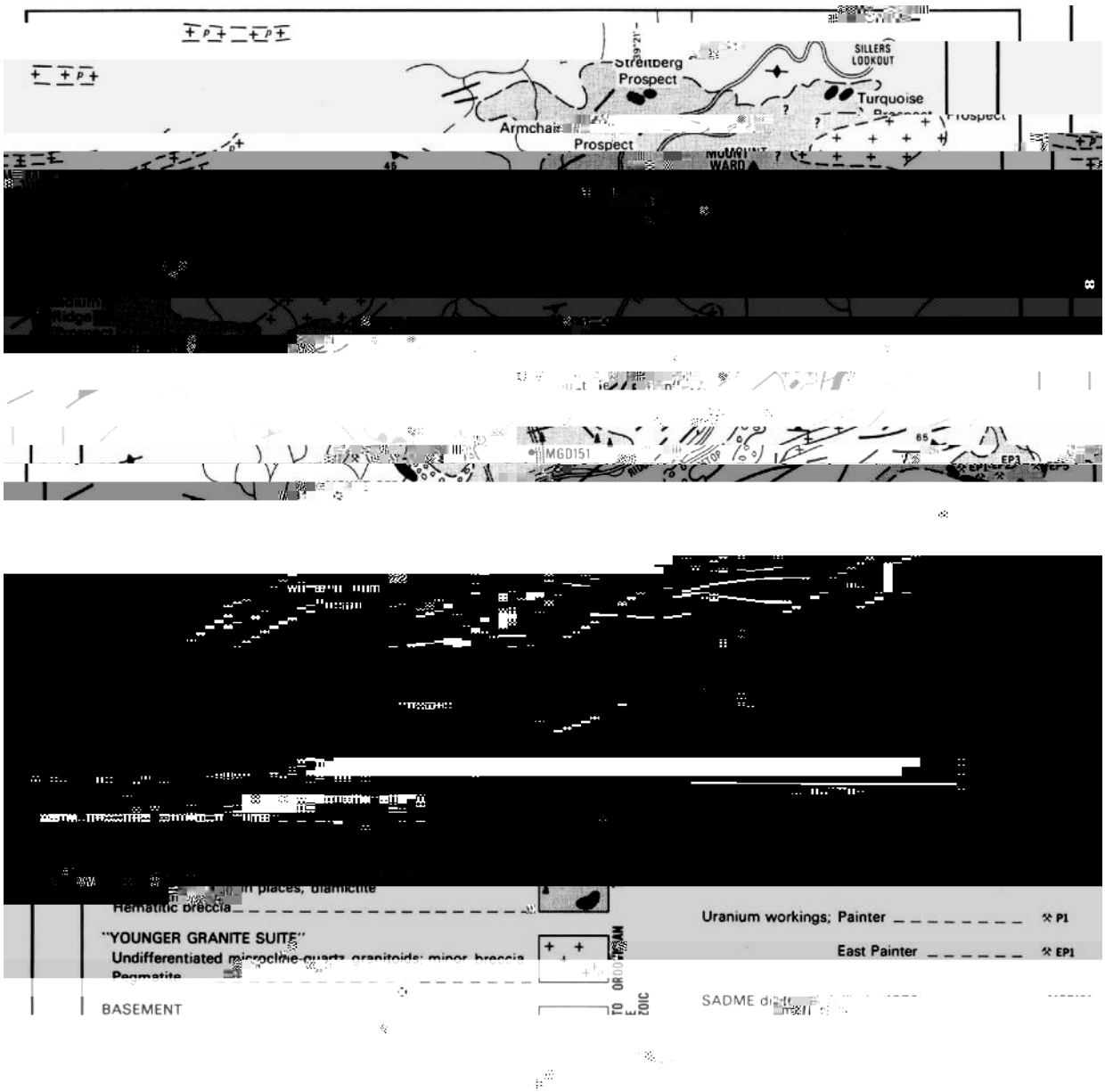

FIG. 3. Geology of the Mount Painter and Mount Babbage Inliers. The various suites are

Mesoproterozoic metasediments and metavolcanics (the Radium Creek Metamorphics), and Mesoproterozoic granites, pegmatites, and minor amphibolite dykes. Ordovician granites and pegmatites make up a "younger granite suite," which intrudes into the Proterozoic basement. The third component is a convoluted and puzzling collection of breccias, of which a granitic breccia is the most common (Fig. 3). Many of these breccias contain uranium and minor sulfide mineralization and are cemented with hematite. The breccias occur as irregular bodies within the basement complex, adjacent to a zone of extensive faulting, which also contains Ordovician granites and pegmatites (Lambert et al., 1982). The breccias have been assigned an age of 280 Ma using palaeomagnetic dating methods (Idnurum and Heinrich, 1993).

A fault system, the Paralana Fault zone, consisting of northeast-trending faults, runs along the eastern margin of the Mount Painter Inlier (Fig. 3). The Paralana Fault zone is generally believed to be the main conduit for hydrothermal fluid dispersal. The fault zone has been intermit-

The PIMA data were collected to provide ground-truthing for the airborne data, which were collected using a PROBE-1 instrument. The main differences between the two instruments are listed in Table 3.

PIMA field spectral measurements were made, and hand-samples were collected of rocks that displayed typical mineralogy for each major outcrop area. A total of 78 spectra were obtained from 60 samples. Preliminary processing was carried out in the field using PIMA View software on a Palmtop computer. Background spectra were removed to obtain hull-quotient spectra that could then be used to determine the second-derivative spectra to enhance spectral features and facilitate preliminary identification of

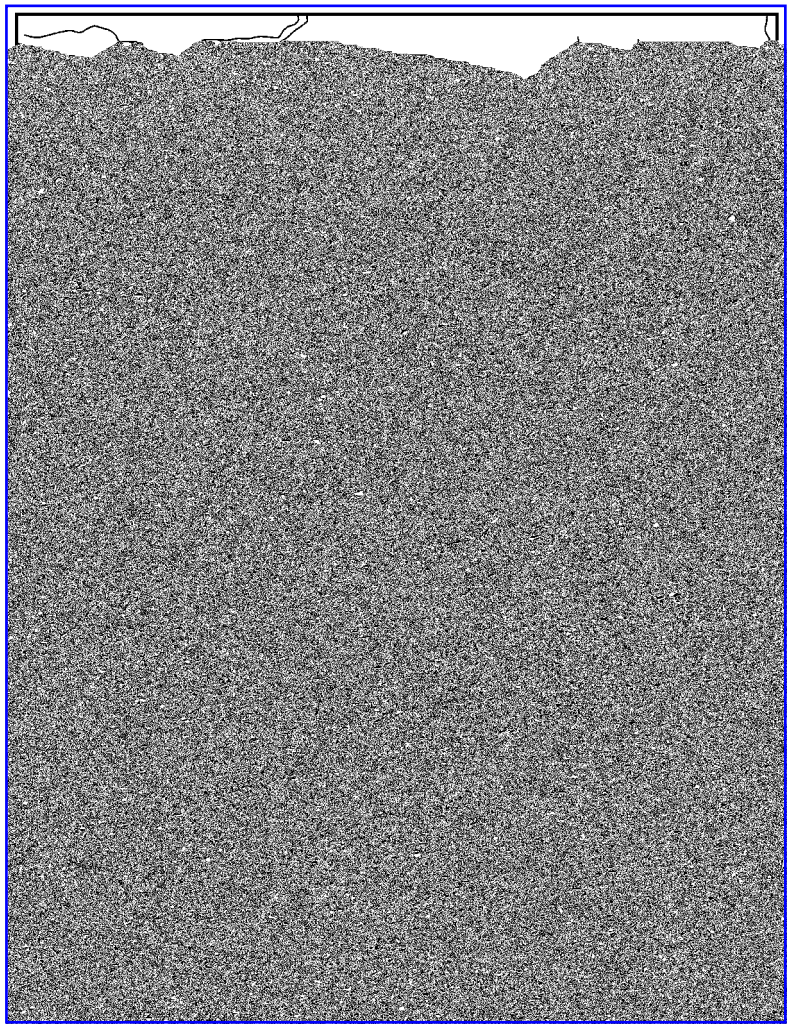

FIG. 5. Location of PROBE-1 data swaths, each 3.2 km wide. The survey was flown in a north–east/south–west direction.

4. Hyper pixel purity index for spatial data reduction—finds spectrally purest pixels in the data by making repeated projections in n-dimensional scatter plots onto a lower-dimensional subspace
5. n-dimensional visualizer rotates the pixels through n-dimensions, producing an animated data cloud by random projections of n-dimensional space; end-members found and identified
6. Creation of regions of interest (ROIs)
7. Creation of spectral library of end-members representing the spectrally purest pixels
8. Location of known material in an unknown background—mixture-tuned matched filtering
9. Redefinition of ROIs based on low infeasibility and high matched filtering scores (gives distribution and abundance maps for end-members)
10. Make ROI masks—one for each end-member
11. Vectorization of ROIs using CSIRO's in-house custom mask creation program designed specifically to automate the creation of vectors from ROIs
12. Selection and arrangement of vector layers of end-members to be shown on the final map

The mineral compositional end-member distributions are superimposed onto a base image (a SWIR band) to provide a reference to the ground surface. Like the PIMA, PROBE-1 provides enough resolution to differentiate between types of micas. Comparisons with PIMA data were used to check these minor spectral variations to see if they had geological significance. In Swath

3, a ring-like structure displays a muted spectrum, similar

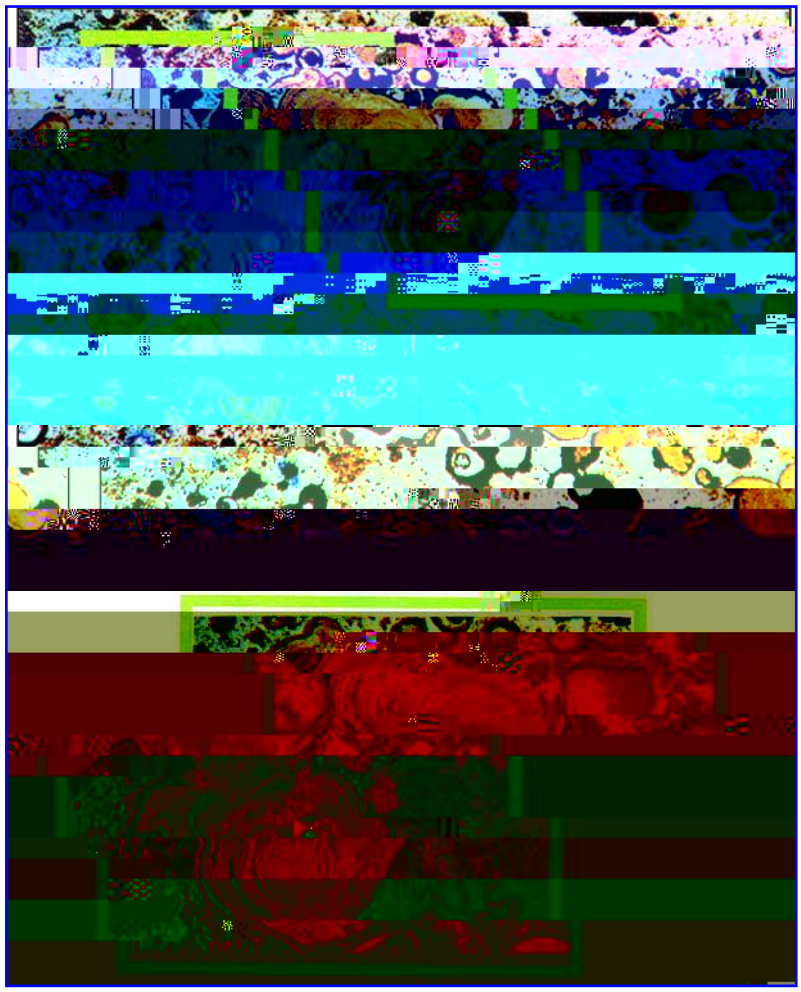

Route starts at southern flank behind and below 5111.1. Scale is approximate only.

side of Mount Painter (see Fig. 7 for location). This outcrop, only some 4–5 m^2, has not previously been reported. Three samples were collected, spectrally analyzed, and thin-sectioned. Analysis of the PIMA data using The Spectral Geologist software registered "null," because the principal rock component is quartz, which has no diagnostic spectral feature at PIMA wavelengths. Petrographic study of two of the samples revealed extensive recrystallization of silica (probably

with values expected for precipitation from fluids derived from argillaceous (carbonaceous) metasediments, as a

FIG. 8. Mount Painter spectra and endmember


b
swath 4
N

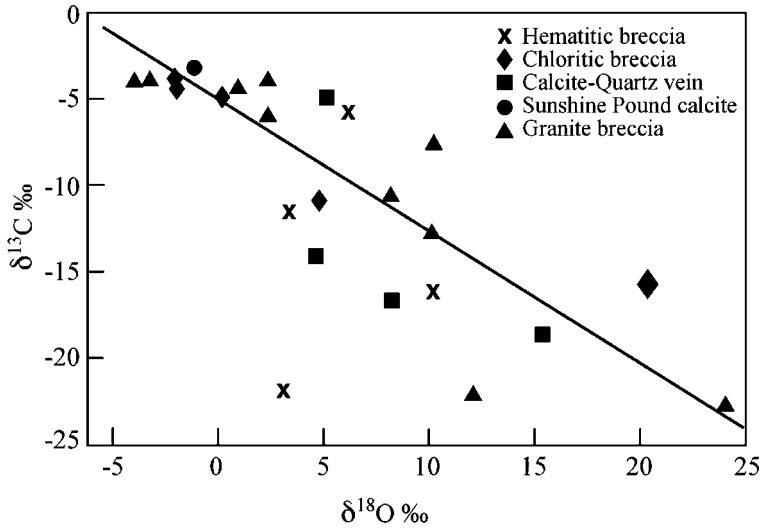
Hematitic breccia
Chloritic breccia
Calcite-Quartz vein
Sunshine Pound calcite
Granite breccia
0
-5
-10
-15
-20
-25
δ13C ‰
-5
0
5
10
15
20
25
δ18O ‰

enhance the unique spectral features at Sinus Meridiani the average neighboring spectrum was removed. The depth and shape of the fundamental bands indicate that the hematite is crystalline and relatively coarse-grained (. 5–10 mm) and thus separate from the fine-grained (diameter , 5–10 mm), red, crystalline hematite that is considered to be a minor spectral component in Martian bright regions like Olympus-Amazonis (Morris et al., 1997; Cristensen et al., 2000).

The large hematite deposit at Sinus Meridiani could have been deposited from hydrothermal fluids. The deposit may represent a deposit formed by an ancient thermal plume, which periodically welled up at the surface. The phenomenon responsible for the vast size of Martian volcanoes, like Olympus Mons, is the apparent lack of plate tectonics. This same phenomenon could also be used to explain the very large size of the proposed hematite deposit at Sinus Meridiani. Other candidates for hydrothermal deposits have also been recognized (Cady and Farmer, 1996).

CONCLUSIONS

Integrated analysis of both air- and ground-collected SWIR hyperspectral measurements can be applied to interpreting hydrothermal alteration in arid regions of Australia. This study suggests that it would also be possible to apply similar techniques to searching for hydrothermal alteration products on the surface of Mars. Current technology is already at a level where airborne or spaceborne hyperspectral measurements of Mars could be collected and would produce similar levels of detail about surface mineralogy as in this study.

Mapping ancient hydrothermal systems with hyperspectral imaging techniques is effective and can provide detailed information. The ability to map minor spectral features in alteration assemblages can identify structures that would be difficult to locate using other techniques. The hyperspectral maps produced show distinctive areas of mineralization commonly associated with the Paralana Fault zone. The Paralana Fault zone

FIG. 10. Low Sulfidation Gold Classification and Fluid Flow Model. From Corbett and Leach (1994).

is

Eugster, H.P. and Jones, B.F. (1967) Gels composed of sodium–aluminum silicate, Lake Magadi, Kenya. Science 161, 160–163.
Foster, D.A., Murphy, J.M., and Gleadow, J.W. (1994) Middle Tertiary hydrothermal activity and uplift of the northern Flinders Ranges, South Australia: insights from apatite fission-track thermochronology. Aust. J. Earth Sci. 41, 11–17.
Fournier, R.O., Thompson, J.M., Cunningham, C.G., and Hutchinson, R.A. (1991) Conditions leading to

This article has been cited by:

"# $%&'() *# +,%-. /%,0(12&'34-!5(678,. *)49(&:4, ; # <0=)4,. >%,:46 ?4,&2&:4-!@A(-# BC""# D(74,074 17(E0)07F
0& 734 5,464&'4 8G +3,8H(74# *Spectroscopy Letters* 44IJ!K. LMN!LMM# 0+,866P4GQ

B# $8R) S,%==4,. 504,,4!*)(0& TU)64,. $83& ?8:4&# BC""# <4&4606 (&: 5,464,V(708& 8G (W,(&0%H!P0'3 5()48-80'